Surface Deposition and Phase Behavior of Oppositely Charged Polyion−Surfactant Ion Complexes. 2. A Means to Deliver Silicone Oil to Hydrophilic Surfaces

Anna V. Svensson,*,† Eric S. Johnson,‡ Tommy Nylander,† and Lennart Piculell†

Division of Physical Chemistry 1, Center for Chemistry and Chemical Engineering, Lund University, POB 124, SE-221 00 Lund, Sweden, and Procter & Gamble Beauty & Grooming, Sharon Woods Technical Center, 11511 Reed Hartman Highway, Cincinnati, Ohio 45241-2422

ABSTRACT The delivery of emulsified silicone oil to hydrophilic silica surfaces by mixtures of cationic polysaccharides and SDS has been studied by in situ null ellipsometry, dynamic light scattering, and turbidity measurements. The emulsion contained silicone oil droplets with a hydrodynamic radius of 18 nm, stabilized by anionic and nonionic surfactants. The investigated polysaccharides were cat-guar and cat-HEC. Both polyions have qualitatively similar adsorption and bulk properties in mixtures with surfactant and emulsion droplets, and both are able to deliver emulsion droplets to the hydrophilic silica surface under suitable conditions. However, there are important quantitative differences that are attributed to a more hydrophobic character of cat-HEC than of cat-guar. The differences in hydrophobicity affect the adsorption from polyelectrolyte/emulsion/surfactant mixtures to hydrophilic silica, especially when an initially surfactant-rich mixture is brought toward phase separation by dilution. Under these conditions, adsorption is obtained only for mixtures with cat-guar. Dynamic light scattering performed on the bulk solutions reveals different aggregation behavior of the cat-guar and the cat-HEC with the silicone oil droplets in the studied surfactant concentration range and the results agree with findings from the adsorption study. Adsorption during dilution of a polyelectrolyte−surfactant mixed solution in the presence of silicone oil droplets gives a larger adsorbed amount and a thicker layer compared to the polyelectrolyte−surfactant mixture without emulsion.

KEYWORDS: polyelectrolyte • surfactant • emulsion • silicone oil • coacervation • cationic • guar • hydroxyethyl cellulose

INTRODUCTION

The deposition of material from a solution to modify the performance of a solid surface is used in a variety of products, such as paints, personal care products, fabric softeners, food products and pharmaceutics. The adsorption is possible if there is an affinity of the matter to the surface. In cases where the material is repelled by the surface, a delivery agent or bridging molecule can be used. In the area of personal care products, silicone oil is often used for surface modification to give a softening feeling to hair and skin (1, 2). The keratin filaments in the outer layer of the skin (stratum corneum) and the hair surface give rise to regions of both hydrophilic and hydrophobic character. Damaged hair is mainly hydrophilic.

In a previous paper, we established the relation between surface deposition and phase behavior of oppositely charged polyion-surfactant ion complexes (3). Here we will exploit the gained knowledge on surface deposition and phase behavior of oppositely charged polyion−surfactant ion complexes for the delivery of silicone oil to a hydrophilic surface, using silica as the model surface. The silicone oil is added as an emulsion stabilized by anionic and nonionic surfactants. Because the model surface (as well as the hair surface) is anionic, it repels the anionic emulsion droplets (4, 5). A cationic polymer, which adsorbs both to the anionic droplets and the anionic silica, can be used as a bridging delivery agent (6–8). In hair care and fabric care contexts, a typical delivery formulation contains, in addition to silicone oil emulsions and cationic polymers, a large amount of anionic surfactant (7). This anionic surfactant binds in excess to the cationic polymer, making the polyion−surfactant complexes net negatively charged. The original formulation is a stable colloidal dispersion, because the polyion−surfactant ion complexes and the surfactant-stabilized emulsion droplets repel each other. On dilution, however, the bulk concentration of surfactant decreases, and surfactant ions therefore leave the polyion−surfactant ion complexes in order to satisfy the binding isotherm. Eventually, the net charge of the complexes becomes sufficiently low so that the stability of the dispersion decreases which in turn leads to association of cationic polymers, surfactant aggregates and silicone oil droplets, both in the bulk and at the surfaces in contact with the formulation. From the perspective of delivery applications, a major challenge is obviously to control these different association processes in order to obtain an efficient delivery of the silicone oil to the target surface. A number of parameters are here important, including both the com-

* Corresponding author. Present affiliation: Danish Technological Institute. E-mail: anna.svensson@teknologisk.dk. Tel.: +45 72 20 24 77.
Received for review September 16, 2009 and accepted December 5, 2009
† Lund University.
‡ Proctor & Gamble Beauty & Grooming.
DOI: 10.1021/am9006319

Table 1. Investigated Polyelectrolytes

name	purification procedure	abbreviation	MW (g/mol)	CD (meq/g)
guar hydroxypropyl trimethylammonium chloride	centrifugation + precipitation in iso-propanol	Cat-guar	2 000 000[a]	0.6[b]
trimethylammonium hydroxyethyl cellulose chloride	dialysis	Cat-HEC LR30M	1 000 000[a]	0.6[b]
trimethylammonium hydroxyethyl cellulose chloride	dialysis	Cat-HEC LR400	400 000[a]	0.6[b]

[a] Weight-average molar mass from GPC-LS. [b] Charge density measured as meq of nitrogen/g of polyelectrolyte.

position and the physical properties of the surfactants and polyions in the formulation.

In our previous paper, we compared two commonly used cationically modified polysaccharide derivatives, cationic guar (cat-guar) and cationic hydroxyethyl cellulose (cat-HEC), using a number of techniques; phase studies, turbidity measurements, dynamic light scattering, gel swelling experiments and in situ null-ellipsometry (3). A consistent picture emerged from these experiments, showing clear similarities between the bulk phase behavior and surface deposition for each studied system, on increasing the surfactant concentration. Interestingly, however, there were important quantitative differences between the two polysaccharides. The cat-guar/surfactant mixtures generally had larger precipitation regions and gave rise to larger adsorbed amounts on silica compared to mixtures with cat-HEC of a similar charge density. These observed quantitative differences were explained by a difference in hydrophobicity of the cationic polysaccharides. For cat-guar, there was a comparatively weak hydrophobic polyion-surfactant attraction. This resulted in a very gradual binding of excess surfactant, resulting in an unusually large phase separation region. For the more hydrophobic cat-HEC, on the other hand, the redissolution of the polyion−surfactant ion complex by excess surfactant took place at much lower surfactant concentration because of a stronger hydrophobic interaction between the surfactant and the polyion.

In the present study, we exploit the gained knowledge to understand the delivery of a silicone emulsion to silica surfaces, using cat-guar and cat-HEC in mixtures with sodium dodecyl sulfate (SDS). The adsorption is studied by in situ ellipsometry. The behavior in bulk is investigated by turbidity measurements and dynamic light scattering. The following main questions are addressed: (1) What is the influence of the emulsion droplets on the phase stability/surface deposition of a polyelectrolyte−surfactant formulation? (2) How do the previously observed differences between cat-guar and cat-HEC affect the deposition of silicone oil droplets, by polyion-surfactant complexes, to a model hydrophilic surface? (3) On deposition by dilution, what are the consequences of the excess surfactant concentration for an efficient deposition?

EXPERIMENTAL SECTION

Materials. Guar grafted with hydroxypropyl trimethylammonium chloride (cat-guar) was supplied by Hercules Incorporated, see Table 1. Samples of hydroxyethylcellulose grafted with hydroxyethyl trimethylammonium chloride (cat-HEC) were supplied by Amerchol Corporation: UCARE polymer LR-30 M and UCARE polymer LR-400. Schematic pictures of the repeating units of the polyions are shown in Figure 1. The polysaccharides

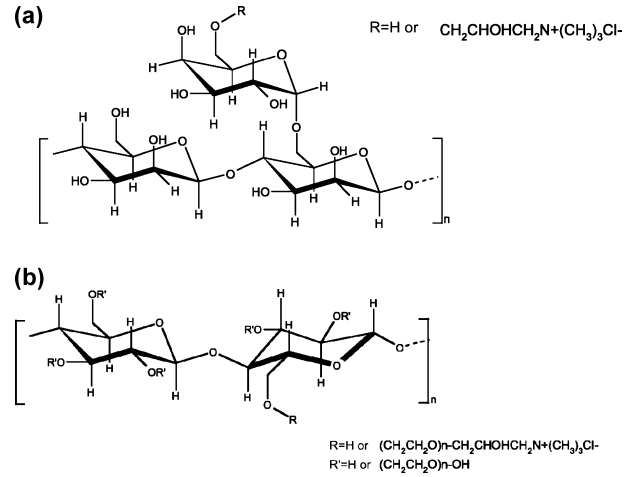

FIGURE 1. Schematic pictures of the repeating unit in (a) cat-guar, (b) cat-HEC.

were purified in order to remove small, water-soluble molecules such as salts and, in the case of cat-guar, water-insoluble material and proteins.

The purification of cat-HEC was made by dialysis with Millipore (MP) water. The dialysis was performed using an Ultrasette tangential flow device from Filtron Technology Corporation. One weight percent polyelectrolyte solution was prepared and pumped through the device with MP water in the other circuit. The nominal molecular weight cutoff of the filter was 10 000. The dialysis was stopped after 24 h when the outgoing "waste" water had reached low conductivity (<2 μS/cm). The dialyzed cat-HEC solution was freeze-dried. Industrial grade guar gum typically contains 4−6% protein and 2.5−5.5% acid-insoluble material originating from the plant seeds from which the guar has been extracted (9). The purification of cat-guar was here made in two steps. The first step involved centrifugation of the translucent solution of unpurified cat-guar to remove water-insoluble material. One g of unpurified cat-guar in 200 mL of MP water was stirred for 24 h. The solution was centrifuged at 20 000*g* for 2 h, and 15 wt % of the original material ended up in a gel-like bottom phase. The transparent supernatant was separated from the bottom phase. The second step was to precipitate the polyelectrolyte. The supernatant solution was poured into iso-propanol (volume ratio 1:9) and the precipitated polyelectrolyte was collected with a stick. The precipitation in isopropanol was repeated 3 times. The thus received purified cat-guar was dried in a vacuum oven at 40 °C. The purified cat-guar was completely water-soluble and gave transparent aqueous solutions.

Elemental analysis of carbon, hydrogen and nitrogen was performed on dry samples of the purified polyelectrolytes to determine the polyion charge density, see Table 1. The amount of protein residues in the cat-guar samples was estimated by a BCA (bicinchoninic acid) assay, see ref 3. The protein content in the purified cat-guar was 1.6 wt %, which implies that roughly half of the protein content was removed by the purification procedure. Because some protein remains after purification, the nitrogen content of cat-guar (0.6 meq/g) may be regarded as an upper limit to the true charge density of purified cat-guar.

Table 2. Contents of the emulsion (45 wt % dry weight)

name	abbr	type of chemical	content (wt %)	concentration (mM)	cmc (mM)
water			55		
polydimethylsiloxane	PDMS	silicone oil, polymer	22		
triethanolamine (TEA) dodecylbenzene sulfonate	$C_{12}BS$	anionic surfactant	14	290	0.15[a]
polyoxyethylene 23 lauryl ether	$C_{12}E_{23}$	nonionic surfactant	6	50	0.06
octamethylcyclotetrasiloxane	OMCTS	silicone oil, tetramer	3	100	

[a] Sodium dodecylbenzene sulfonate.

The complete removal of boron during the purification of cat-guar, originally present in the cat-guar as Borax, was confirmed by elemental analysis of boron. The cited molecular weights were determined by gel permeation chromatography coupled with light scattering (GPC-LS).

The silicone oil emulsion was from Dow Corning and the composition is shown in Table 2. The concentration of the emulsion will be given either as the total dry weight percent, or as the concentration of the anionic surfactant in the emulsion, i.e., the triethanolamine-dodecylbenzene sulfonate ($C_{12}BS$).

Sodium dodecylsulfate (SDS) was supplied from BDH (powder). Triethanolamine dodecylbenzene sulfonate ($C_{12}BS$) was from Stepan Co. It was an aqueous solution containing 59.2 wt % $C_{12}BS$ and 2.1 wt % Na_2SO_4. Polyoxyethylene 23 lauryl ether ($C_{12}E_{23}$) was from J.T. Baker and Uniqema (liquid). The surfactants were used without further purification. The pH of the investigated mixtures in the study was 6.5. Because triethanolamine (TEA), the counterion of $C_{12}BS$, has a pK_a of 7.8, it was assumed that TEA is protonated and cationic under the experimental conditions used in this study.

Methods. ***In situ Null Ellipsometry.*** An automated Rudolph Research thin-film null ellipsometer type 43603−200E was used to measure the adsorbed amount and the thickness of adsorbed layers in situ. All measurements were performed at a wavelength of 4015 Å, using a xenon lamp with a filter. The substrates used were silicon wafers, which were cut in 12 × 20 mm pieces and thermally oxidized to get a silicon oxide layer with a thickness of 300−350 Å. The substrates were cleaned for 5 min in 25% NH_4OH (pro analysis, Merck), 30% H_2O_2 (pro analysis, Merck), and H_2O (1:1:5 by volume) at 80 °C for 5 min, followed by a mixture of 32% HCl (pro analysis, Merck), 30% H_2O_2 (pro analysis, Merck), and H_2O (1:1:5 by volume) at 80 °C for 10 min, and after thorough rinsing with MP water they were stored in pure ethanol. The silica substrates were dried with nitrogen and then treated in an air (0.001 mbar) plasma cleaner (Harrick Scientific Corp., model PDC-3XG) before the measurements. Hydrophilicity of the surfaces was verified by complete wetting by a droplet of water.

The optical properties of silicon wafer were characterized by the ellipsometer in air and in 1 mM NaCl, which gave information about the thickness and refractive index of the silicon oxide layer and the (complex) refractive index of the silicon (10). A silica surface is negatively charged in water due to the deprotonation of the surface Si−OH groups. The solution in the cuvette was agitated with a magnetic stirrer at about 300 rpm. In the instrument used, the substrate surface is positioned vertically in the ellipsometer cuvette. Consequently, precipitated material, generated under conditions of bulk phase separation, does not settle on the surface by gravity.

In the adsorption experiments, 0.5 mL of a 1000 ppm polyelectrolyte solution was added to the cuvette filled with 4.5 mL of 1 mM NaCl of pH 6.5, yielding a final polyelectrolyte concentration in the cuvette of 100 ppm. Known small amounts of 10, 100, or 500 mM surfactant solutions or emulsion were progressively added to obtain the desired concentrations in the cuvette. The adsorption after each addition was allowed to reach a steady state, which took approximately 2000−3000 s.

In the rinse experiments, 0.5 mL of a mixture of 1000 ppm polyelectrolyte and varied concentration of surfactant, with or without 4000 ppm emulsion, was initially added to the cuvette filled with 4.5 mL of 1 mM NaCl at pH 6.5. The adsorption was measured until a steady state was reached. The solution in the cuvette was then replaced by "rinsing", that is, pumping 1 mM NaCl through an inlet tube connected to the cuvette, under well-defined flow conditions (ca. 6 mL/min). An outlet tube ensured that the volume in the cuvette was kept constant at 5 mL during the rinse. In this way, the bulk solution was gradually replaced by a 1 mM NaCl solution.

The data from the ellipsometry measurement, Ψ and Δ, correspond to the relative amplitude change and the relative phase shift, respectively, upon reflection of polarized light against an interface. A four layer optical model, assuming isotropic layers and planar interfaces, was used to obtain the thickness and refractive index of the adsorbed layer from Ψ and Δ by means of an iterative procedure (10). The adsorbed amount was then calculated by using the values of the thickness and the refractive index of the layer, according to

$$\Gamma = \frac{d_f(n_f - n_0)}{dn/dc} \quad (1)$$

Here Γ is the mass per surface area (mg/m^2), d_f is the thickness of the adsorbed film (*Å*), n_f is the refractive index of the adsorbed film, n_0 is the refractive index of the bulk solution, and *dn/dc* the refractive index increment as a function of the bulk concentration. The *dn/dc* values of the polyelectrolytes were measured by GPC-LS refractive index detector as 0.153 mL/g for the cat-guar and 0.129 mL/g for the cat-HECs. The *dn/dc* value of SDS has been determined to 0.147 in an earlier study (11). Because one cannot resolve the relative contributions to the adsorbed layer from the components by ellipsometry, and the values of *dn/dc* for the different component are quite similar, we used a *dn/dc* value of 0.15 mL/g for all polyelectrolytes, surfactants, and mixtures thereof, including the silicone oil, in the present study (11–13).

UV−Vis Spectrophotometry. The turbidity was determined by absorbance measurements in the visible light region (λ = 500 nm) using a Perkin-Elmer Lambda 14 UV/vis spectrophotometer. PS cuvettes with a path length of 1 cm were used. The conditions in the cuvette during the turbidity measurements were similar to those in the ellipsometry measurements, with stepwise addition of surfactant to a solution of 100 ppm polyelectrolyte. The absorbance was measured 5 min after each surfactant addition, followed by measurements after 10, 20, and 30 min. The cuvette was put on stirring between the measurements.

Dynamic Light Scattering. The setup used for the dynamic light scattering (DLS) of the polyelectrolyte−surfactant−emulsion mixtures was an ALV/DLS/SLS-5000F, CGF-8F-based compact goniometer system from ALV-GmbH, Langen, Germany. The light source is a CW diode-pumped Nd:YAG solid-state Compass-DPSS laser with symmetrizer from COHERENT, Inc., Santa Clara, CA. It operates at 532 nm with a fixed output power of 400 mW. The laser intensity can be modulated by an external

compensated attenuator from Newport Coorporation, California. The instrumental settings are described elsewhere (14). The measuring temperature was set to room temperature. The scattering angle was fixed to 90°.

In the DLS measurements, the time-correlation function (auto or pseudocross) of the scattered intensity is measured. The normalized intensity correlation function $g^{(2)}(t)$ is related to the normalized time correlation function of the electric field $g^{(1)}(t)$ by Siegert's relation: $g^{(2)}(t) - 1 = \beta[g^{(1)}(t)]^2$, where t is the lag time and β (≤ 1) is a coherence factor that accounts for the deviation from ideal correlation and the experimental geometry. For polydisperse particles, or for different modes of motion field, $g^{(1)}(t)$ may be described by

$$g^{(1)}(t) = \int_0^\infty \tau A(\tau)\exp(-t/\tau)d\ln\tau \qquad (2)$$

Here τ is the relaxation time and $A(\tau)$ is the relaxation time distribution. The DLS data were analyzed by regularized inverse Laplace transformation to obtain the relaxation time distribution using the algorithm included in the ALV software. The results are shown as relaxation time distributions, i.e., $\tau A(\tau)$ as a function of $\log(\tau/ms)$, which we have normalized with the maximum peak height.

In the limit of small scattering vectors (q), the apparent translational diffusion coefficient (D_{app}) at finite concentration can be calculated from the relaxation rate (Γ), which is obtained from the first moment of the translational mode in the relaxation time distribution

$$D_{app} = \left(\frac{\Gamma}{q^2}\right)_{q\to 0} \qquad (3)$$

Here $\Gamma = 1/\tau$ and q is the magnitude of the scattering vector [$q = 4\pi n_0 \sin(\theta/2)/\lambda$, where n_0 is the refractive index of water, λ is the incident wavelength, and θ is the scattering angle]. From the apparent translational diffusion coefficient, we obtained the apparent hydrodynamic radius through the Stokes–Einstein relationship as

$$R_H^{app} = \frac{kT}{6\pi\eta_0 D_{app}} \qquad (4)$$

Here k is Boltzmann's constant, T is the absolute temperature, and η_0 is the viscosity of water.

The samples for the DLS measurements were prepared in the following way. The solvent, 1 mM NaCl, was filtered through a 0.1 μm filter. Appropriate amounts of polyelectrolyte, surfactant, emulsion, and solvent were weighed in a glass container and sealed with a cap. The sample was shaken by hand and by Vortex mixer. It was put on a tilting plate for 24 h, or longer if the sample was not yet homogeneous. The sample was centrifuged at 3000 rpm for 1 h to remove dust particles that might otherwise disturb the DLS measurements. The top part of the sample was transferred with a syringe to the glass tube for the DLS measurement.

RESULTS

Interactions between the Cationic Polymers and SDS. First we studied the emulsion-free mixtures of the cationic polymers with SDS. Figure 2 shows the adsorption and turbidity of the cationic polymers during progressive addition of SDS. For the convenience of the reader the data for cat-guar and cat-HEC LR30 M are reproduced from our previous study (3), but we have in the present investigation included also cat-HEC LR400. All cationic polyions have similar charge densities, but differ in molecular weight (Table 1). Panels a and b in Figure 2 show the adsorbed amount and the layer thickness on hydrophilic (anionic) silica. All polyions adsorb to hydrophilic silica. In the absence of added surfactant, the adsorbed amount of LR30 M was 1.0 mg/m^2, followed by LR400 and cat-guar at 0.6 mg/m^2. The adsorbed amount increased during the addition of surfactant, and a maximum occurred at 2 mM SDS for the two cat-HEC polyions and at 5 mM for the cat-guar. At higher SDS concentrations, the adsorbed layer swelled due to an over-

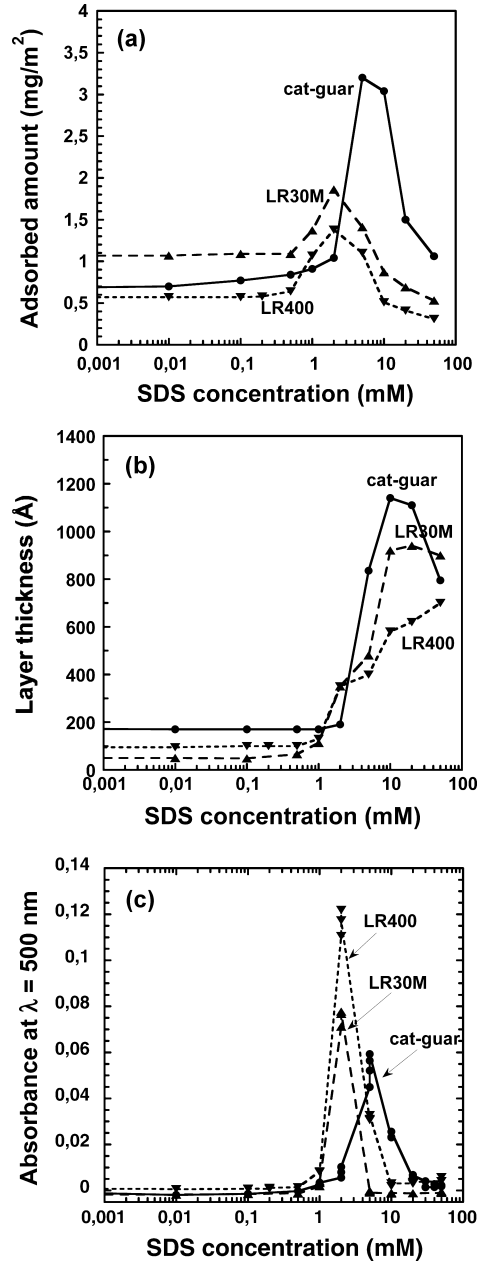

FIGURE 2. Adsorption and bulk phase separation of 100 ppm polyelectrolyte solutions on stepwise addition of SDS. (a) Adsorbed amount and (b) thickness of the adsorbed layer on hydrophilic silica. (c) Turbidity in the bulk solution (purified cat-guar = circles/solid line, LR30 M = triangles/hatched line, LR400 = inverse triangles/dotted line).

charging of the complex by excess surfactant and desorption takes place, see Figure 2b. The cat-guar/SDS layer swelled to 120 nm, but decreased slightly because of desorption at higher SDS concentrations. The cat-HEC/SDS layers swelled to 90 nm (LR30M) and 70 nm (LR400), respectively.

Figure 2c shows the variation in turbidity in the bulk solution, which closely follows the adsorption behavior. An increased turbidity signifies a phase separation of polyion−surfactant ion complexes. The progressive addition of SDS gave rise to turbidity maxima at the same SDS concentrations as the adsorption maxima in Figure 2a.

Characterization of the Emulsion Droplets. The emulsion contained silicone oil droplets stabilized by the anionic surfactant triethanolamine dodecylbenzene sulfonate (C_{12}BS) and the nonionic surfactant polyoxyethylene 23 lauryl ether ($C_{12}E_{23}$). Table 2 shows the composition of the emulsion. The weight ratio of oil vs surfactants was 1:0.8, and the molar ratio of anionic vs nonionic surfactant was 1:0.2. The apparent hydrodynamic radius of the droplets, as obtained from DLS (see below), was 18 nm. Using this value and a density of 1 g/cm^3 for the droplets, made up of silicone oil and the surfactants, the surface area per surfactant molecule is calculated to 0.4 nm^2 if we assume that all surfactant adsorbs to the surface of the droplets. This value is roughly as (or slightly larger than) expected for a surfactant monolayer, suggesting that there is just enough of surfactant molecules in the emulsion to cover the surface of the oil droplets. The number of surfactant molecules per silicone droplet is ca. 10 000, of which 85% are anionic. Also considering the high affinity of the surfactant toward a hydrophobic surface, it is therefore likely that most of the surfactant is located on the silicone oil droplets. We should, however, keep in mind that the radius obtained from DLS is a hydrodynamic radius and, moreover, a *z*-average of a distribution of particle radii. Thus we can expect to obtain only a rough estimate of the true specific area of the droplets based on this value.

The stability of the emulsion was investigated with respect to dilution with water and addition of SDS, respectively. Figure 3a shows the relaxation time distributions from DLS measurements on the emulsion at various degrees of dilution with water. The emulsion was translucent at high concentrations, but was sufficiently transparent for DLS measurements when diluted (<1 wt %). The droplet radius was maintained at 17−18 nm during dilution. Figure 3b shows the relaxation time distribution at increasing concentrations of SDS. Again, the droplet size stayed around 18 nm, even at very high SDS concentrations, up to 50 mM. It should be noted that the samples were prepared by gentle mixing on a tilting table for a couple of days. No extra energy was put into the system, and as expected the size of the silicone oil droplets were therefore maintained on adding large concentrations of SDS, which for coarser emulsions would favor a decrease in droplet size. This suggests an effective kinetic stabilization presumably due to the polymeric nature of the emulsified silicone oil.

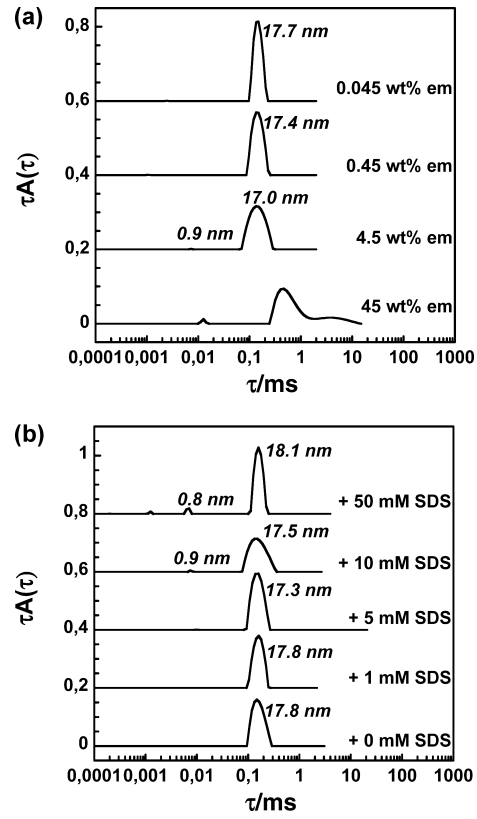

FIGURE 3. Relaxation time distributions at $\theta = 90°$ for a) the emulsion during dilution with water (from bottom: 45, 4.5, 0.45, 0.045 wt %), and (b) 0.04 wt % emulsion during the addition of SDS (from bottom: 0, 1, 5, 10, and 50 mM SDS). The apparent hydrodynamic radius as calculated from the Stokes−Einstein relationship (eq 4) is also inserted.

To further investigate the stability of the emulsion, we put samples of various concentrations either in the freezer (−15 °C) or in a thermoblock (70 °C) for 2 days. After equilibration at room temperature for 7 days, the samples were investigated by DLS (data not shown). The hydrodynamic radius of the silicone droplets was still 17−18 nm, implying that either the droplets survived the thermal treatment without changing their size, or that the system, after some change in the droplet size, managed to return to its original state after the temperature quenching. As we shall see below, the remarkable insensitivity of the size of the silicone oil droplets to various kinds of treatment of the emulsions turned out to be very advantageous for the interpretation of our experimental results.

Interactions of cat-HEC with Components from the Emulsion. The interactions between cat-HEC LR30 M and the emulsion components were investigated by studying mixtures of the polyion with different types of anionic aggregates related to the emulsion. In addition to mixtures with the full emulsion, mixtures of LR30 M with only the anionic surfactant from the emulsion (C_{12}BS), or with the anionic and the nonionic surfactant (C_{12}BS/$C_{12}E_{23}$ mix) were studied. The molar ratio in the C_{12}BS/$C_{12}E_{23}$ mix was 1:0.2, i.e. the same as in the emulsion. Figure 4 shows the adsorption and the turbidity of LR30 M in mixtures with C_{12}BS, C_{12}BS/$C_{12}E_{23}$ mix, or the full emulsion, respectively. The solution contained 100 ppm polyelectrolyte. The ad-

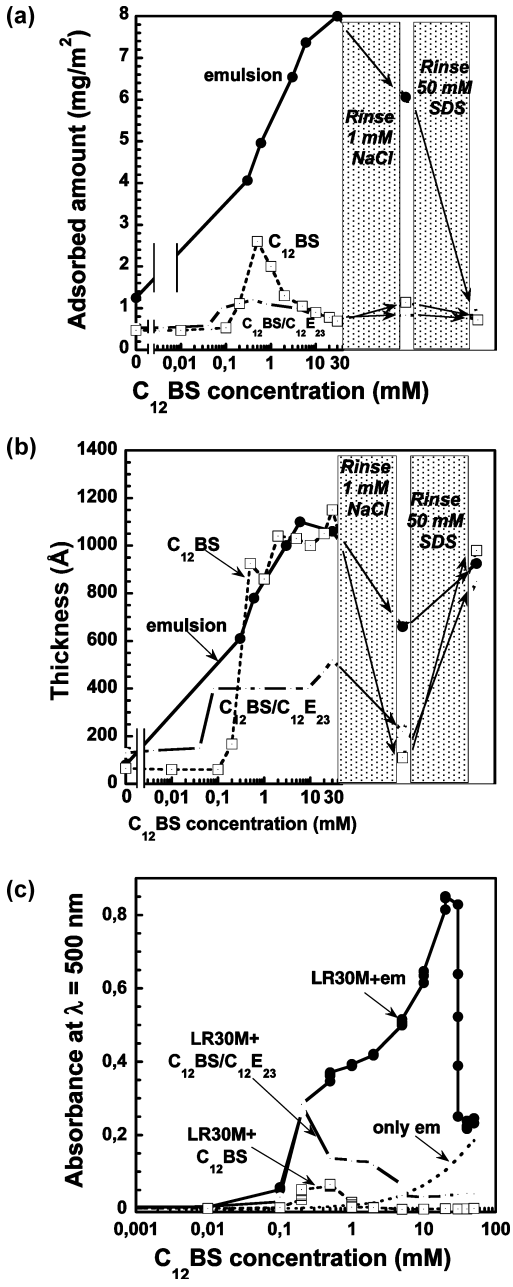

FIGURE 4. Adsorption and bulk behavior during the addition of emulsion (filled circles/solid line), a $C_{12}BS/C_{12}E_{23}$ mix with molar ratio 1:0.2 (circles/hatched line) or $C_{12}BS$ alone (squares/dotted line). The start solution contained 100 ppm LR30M. (a) Adsorbed amount on silica, (b) thickness of the adsorbed layer on silica, and (c) turbidity of the bulk solution. The data are plotted versus the concentration of $C_{12}BS$. The last points in a and b show the effect on the adsorbed layer after rinsing with 1 mM NaCl, followed by rinsing with 50 mM SDS.

sorbed amount and the layer thickness on hydrophilic silica as a function of the concentration of added $C_{12}BS$ are shown in panels a and b in Figure 4. The corresponding turbidity of the bulk is shown in Figure 4c. The *x*-axis is in all cases given as the concentration of $C_{12}BS$ in the mixtures.

We will now consider the effect of additives one at a time, stepwise increasing the complexity of the system. The addition of the $C_{12}BS$ alone gave rise to a variation in adsorption, similar to the behavior observed with SDS (shown in Figure 2 above). An increase in adsorbed amount and layer thickness started at 0.1 mM $C_{12}BS$, see Figure 4a,b, and the adsorbed amount reached a maximum value of 2.5 mg/m^2 at 0.5 mM $C_{12}BS$. The adsorbed amount decreased at higher surfactant concentrations, and a swelling of the layer to a thickness of 100 nm was observed. The turbidity in the bulk closely followed the adsorption behavior with a maximum at 0.5 mM $C_{12}BS$, see Figure 4c.

There was a similar nonmonotonic variation in adsorption and turbidity with the progressive addition of the $C_{12}BS/C_{12}E_{23}$ mix, see Figure 4a–c, but with broader maxima. The increase in adsorption started at a $C_{12}BS$ concentration of 0.05 mM, which was lower than for the pure $C_{12}BS$ surfactant. The following maximum in adsorbed amount was broader than for $C_{12}BS$ alone, but reached only 1.2 mg/m^2. At high surfactant concentrations, the swollen layer had a thickness of roughly 50 nm. Again, the turbidity results closely followed the adsorption results.

Figure 4a shows that the addition of the full emulsion gave rise to a huge increase in adsorbed amount; up to 8 mg/m^2 at the highest possible addition in the ellipsometer cuvette, which was 4.5 wt % emulsion (corresponding to 30 mM $C_{12}BS$) with the used experimental protocol (see Experimental Section). The layer thickness at the adsorption maximum was 100 nm, that is, similar to that observed for adding only the anionic surfactant to the cat-HEC solution, see Figure 4b. The ellipsometer measurement at the highest emulsion content was made with some difficulty because of scattering of light in the cuvette, caused by phase separation in the bulk. The adsorbed amount at this point showed a small decrease with time (not shown), leveling off at 8 mg/m^2. This suggests that there may be a maximum in adsorbed amount close to this emulsion content. This conclusion is supported by the turbidity measurements in Figure 4c, which were extended to higher emulsion contents than the adsorption measurements. The turbidity increased until an emulsion content equivalent to 20 mM $C_{12}BS$ was reached. At 30 mM $C_{12}BS$, the turbidity suddenly dropped dramatically with time and, with further additions of emulsion, approached a value similar to the turbidity of the pure emulsion.

Sequential Dilution of Bulk Solution with NaCl and SDS. After the maximum concentration of additives was reached at a $C_{12}BS$ concentration of 30 mM, the cuvette content was diluted and the effect on the adsorbed layer was recorded by ellipsometry, see Figure 4a,b. The aim was to determine to what extent the various components in the deposited layers could be removed by the dilution or rinsing step, first with only the "background" dilute electrolyte solution (1 mM NaCl), and then with a harsher detergent solution (50 mM SDS), which could be expected to more efficiently remove adsorbed components from the surface. Rinsing with the dilute salt solution induced a collapse of the swollen layers in all cases (Figure 4b), whereas the variation in adsorbed amount (Figure 4a) was different for the different combinations of additives. There were small or no changes in the adsorbed amount for $C_{12}BS$ alone or the surfactant mix, but a significant desorption for the full emulsion. Still, the adsorbed amount remained high

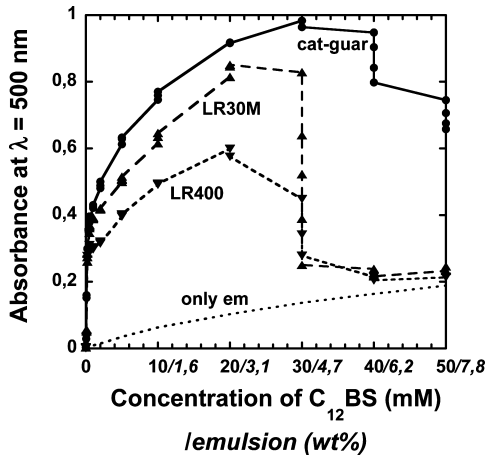

FIGURE 5. Turbidity as a function of the concentration of stepwise added silicone emulsion to a 100 ppm polyelectrolyte solution (cat-guar = circles/solid line, cat-HEC LR30 M = triangles/hatched line, cat-HEC LR400 = inverse triangles/dotted line). The data are plotted versus the concentration of C_{12}BS (mM) and the concentration of emulsion (wt %). The turbidity of the emulsion alone is also shown (dotted line).

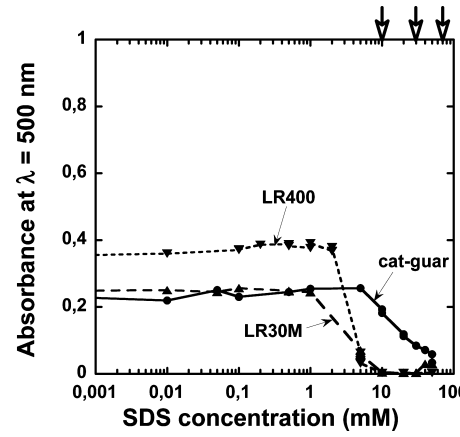

FIGURE 6. Turbidity as a function of the concentration of SDS added stepwise to 100 ppm polyelectrolyte/400 ppm emulsion (cat-guar = circles/solid line, cat-HEC LR30 M = triangles/hatched line, cat-HEC LR400 = inverse triangles/dotted line). Thick arrows indicate the compositions of mixtures used in the rinse experiments, see text.

for the surface treated with the full emulsion, indicating that only a minor fraction of the emulsion droplets could be removed by rinsing with a dilute salt solution. Interestingly, when the dilute salt solution was replaced by 50 mM SDS, the results on rinsing for all systems converged to virtually identical values with an adsorbed amount of 0.5−0.6 mg/m^2 and a layer thickness swollen to 100 nm. The latter values are very similar to those obtained by progressive addition of SDS alone to a preadsorbed layer of LR30 M up to a level of 50 mM (see Figure 2). In other words, there is no evidence that emulsion droplets remain in the adsorbed layer after rinsing with SDS.

Comparing Different Polyions Mixed with the Emulsion. Figure 5 compares the turbidities of the various polyion solutions as a function of the amount of added emulsion. The emulsion concentration is again given as the concentration of C_{12}BS, and the solution contains 100 ppm polyelectrolyte. The data for LR30 M are the same as in Figure 4. Note that the *x*-axis in Figure 5 has a linear scale, because we want to highlight the dissolution processes occurring at high amounts of emulsion. The turbidity of the polysaccharide/emulsion mixtures increases continuously with the amount of added emulsion to reach a pronounced maximum, followed by sharp drop in turbidity at high emulsion concentrations. The results for the two cat-HECs follow each other closely, but with consistently lower turbidities for LR400. The turbidity drop for the cat-HEC/emulsion mixtures appears at an emulsion content equivalent to 30 mM C_{12}BS. For the cat-guar/emulsion mixture, the turbidity decrease occurs at higher emulsion concentration and is less steep; a clear decrease is first noticed at an emulsion content equivalent to 40 mM C_{12}BS. The magnitude of the turbidity decrease of the cat-guar mixture is not as large as in the cat-HEC cases, and does not approach the level of the pure emulsion in the investigated concentration range (up to 7.8 wt % emulsion, equivalent to 50 mM C_{12}BS).

Turbidity of Formulations including SDS. A simplified model of a hair care formulation is a mixture of cationic polymer, silicone oil, and anionic surfactant. The weight ratio of polyelectrolyte vs silicone oil is typically 1:2. The amount of anionic surfactant is typically 30 times larger than the polyelectrolyte content. In our dilute systems, such a formulation would correspond to a mixture of 100 ppm cationic polymer, 400 ppm emulsion (dry weight) and ca. 3000 ppm, or 10 mM, anionic surfactant (SDS). To elucidate the behavior of such a composition, SDS was progressively added to premixed samples of 100 ppm polyelectrolyte and 400 ppm emulsion during stirring. At a certain amount of SDS, the large particles of concentrated phase, giving rise to a turbid solution, started to dissolve, and with a progressive addition of more SDS the mixtures finally became clear. Figure 6 shows the turbidity in the polyelectrolyte/emulsion mixtures as a function of the added SDS. In both cat-HEC/emulsion mixtures, there was a turbidity drop at SDS concentrations below 10 mM, with most of the drop occurring below 5 mM SDS. In the cat-guar/emulsions, the turbidity decreased much more gradually, starting above 5 mM SDS with a significant turbidity remaining at the highest concentrations (50 mM) SDS investigated. In a separate phase study, clear solutions were reached at 70 mM SDS (not shown).

We note that the exact history of the sample preparation seems to play a role for the measured turbidity. The samples in Figure 6 were made by direct addition of 400 ppm emulsion to 100 ppm polyelectrolyte and in Figure 6, the LR400 mixture has the highest turbidity, followed by cat-guar and LR30 M, which are equal. The results in Figure 5, on the other hand, were obtained by progressively adding the emulsion to 100 ppm polyelectrolyte, and in the latter experiments, the turbidity was highest for LR30 M and cat-guar, whereas the LR400 gave somewhat lower turbidity. (This ranking held true also at 400 ppm emulsion, even though the results for these low emulsion concentrations are

Table 3. Investigated Mixtures in the Rinse Experiments

	polyelectrolyte (ppm)	emulsion (ppm)	SDS (mM)		
cat-guar	100	400		30	70
LR30M	100	400	10	30	70
LR400	100	400	10		

not visible in Figure 5 because of the linear scale.) Nevertheless, the turbidities of the two systems are of comparable magnitude.

Surface Deposition by Diluting Full Polyelectrolyte/Emulsion/SDS Formulations. Studies of the effect of diluting the bulk solution on the deposited layer were performed on full "hair care formulation" mixtures as described above, to imitate the process of washing. Because ellipsometry measurements are preferably made on transparent or translucent solutions, care was taken to design the experiments so that relevant compositions were investigated without involving too high turbidity. The samples should also represent different starting conditions with respect to the phase behavior of each polyion. On these grounds, the selected initial compositions were 100 ppm polyelectrolyte, 400 ppm emulsion, and SDS concentrations of either 10, 30, or 70 mM, see Table 3. These initial mixtures were in most cases transparent one-phase samples, but the mixtures all reached phase separation upon sufficient dilution, i.e., during rinsing. The three arrows in Figure 6 indicate the selected initial SDS concentrations. At an SDS content of 10 mM, both cat-HEC/emulsion complexes are redissolved, but the systems are quite close to the boundary to the phase-separation region. At an SDS content of 70 mM the cat-guar/emulsion complexes are redissolved, but this system is still close to the boundary to the phase separation region, see above. An SDS concentration of 30 mM represents an intermediate case; inside the phase separation region for the cat-guar system, but well outside the phase separation region for the cat-HEC formulations.

We studied the effect of diluting the bulk solution on the adsorbed layer structure for each polyion with and without the presence of emulsion droplets. In each (rinse) experiment, the adsorption was first followed until steady state was obtained and then the cuvette content was diluted, by flowing 1 mM NaCl through the cuvette.

The results for the LR30 M mixtures are shown in Figure 7, where the changes in adsorbed amount as well as thickness with and without emulsion are compared. No adsorption from the LR30M/10 mM SDS mixtures occurred prior to diluting the content in the cuvette, see Figure 7a. A rapid adsorption occurred during the first minute of rinsing, seen as a sharp increase in the adsorbed amount to 0.5 mg/m^2 and a thickness of 20 nm. A much higher adsorbed amount on rinsing was obtained for the mixture containing emulsion droplets. As the initial SDS concentration was increased, resulting in a system further away from the conditions of phase separation, less adsorption occurred during rinsing. Figure 7b shows the effect of rinsing from mixtures of 100 ppm LR30 M with 30 mM SDS. The steady state adsorbed amount after rinse was 0.5 mg/m^2 without emulsion (bottom plot) and 0.7 mg/m^2 with emulsion (top plot). Figure 7c, finally, shows the results for mixtures with 100 ppm LR30 M and 70 mM SDS. These mixtures gave hardly measurable adsorbed amounts on rinsing, regardless of the presence or absence of emulsion droplets.

The results in terms of thickness and adsorbed amount from dilution of mixtures of 100 ppm LR400 and 10 mM SDS are shown in Figure 8. As for the LR30 M mixtures, there was no adsorption directly after injection. The onset of rinsing induced rapid adsorption, reaching an adsorbed amount of 0.9 mg/m^2 without emulsion and a twice as high adsorbed amount, 1.7 mg/m^2, with emulsion droplets present.

Unlike the cat-HEC systems, the mixtures with cat-guar gave an adsorption directly after injection of the polyelectrolyte/surfactant mixture. The cat-guar/30 mM SDS mixture gave an adsorbed amount of 0.5 mg/m^2, with a layer thickness of 80 nm, before rinse, see Figure 9a. The rinsing induced a small increase in the adsorbed amount and a decrease in the thickness. The corresponding cat-guar mixture with emulsion, i.e., the cat-guar/emulsion/30 mM SDS mixture, was initially too turbid to be measured by ellipsometry. The measurement could only start when the turbid solution had been partly replaced by 1 mM NaCl. The adsorbed amount after rinse was 1.8 mg/m^2 with a layer thickness of 25 nm. We note that the adsorbed amount was strongly increased in the presence of the emulsion droplets in cat-guar/30 mM SDS, but the layer thickness was unchanged.

Figure 9b shows the rinse experiments of cat-guar mixtures containing 70 mM SDS. Adsorption occurred directly after injection, giving an adsorbed amount of 0.7 mg/m^2 in the absence of emulsion droplets. The rinsing gave rise to a small increase in the adsorbed amount, whereas the layer thickness decreased from 30 to 10 nm. The corresponding system with emulsion gave an even higher adsorbed amount, 1.8 mg/m^2 after injection, which increased on rinsing. The layer collapsed during the rinse, seen as a slow decay in the thickness with time during the rinsing process. The layer reached a steady-state thickness of approximately 35 nm.

We note that many of the systems display a more or less pronounced adsorption peak during the initial 300−500 s on rinsing.

Soluble Complexes in Full Polyelectrolyte/Emulsion/SDS Formulations. DLS measurements were made on polyelectrolyte/emulsion/SDS mixtures, with a particular emphasis on conditions corresponding to the initial compositions in the dilution experiments. Generally, the relaxation time distributions showed the presence of one slow and one fast diffusing object, which can be ascribed to larger objects and free surfactant micelles, respectively. Figure 10 shows relaxation time distributions for LR30M/10 mM SDS mixtures, without emulsion (bottom curve) and with emulsion (top curve). The apparent hydrodynamic radius of the emulsion-free polyion-surfactant ion complex was 40 nm. If the emulsion was present in the mixture (top plot), there was a narrowing of the broad peak to a radius of

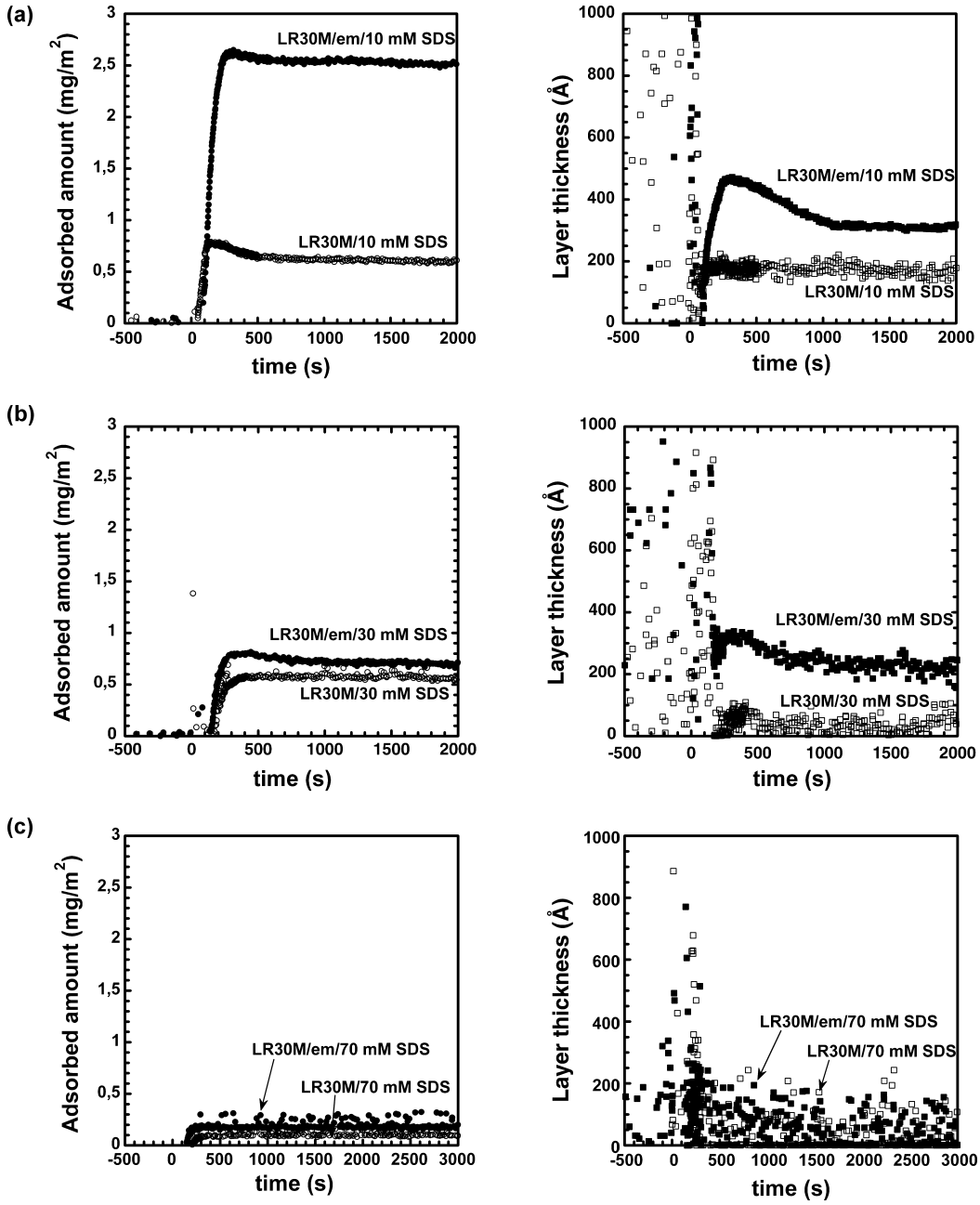

FIGURE 7. Results from adsorption of cat-HEC LR30M/SDS solutions with (filled symbols) or without (unfilled symbols) silicone oil emulsion on silica surface followed by dilution of bulk solution with 1 mM NaCl (rinsing). Initial concentrations were 100 ppm polyelectrolyte, 0 or 400 ppm emulsion, and (a) 10, (b) 30, or (c) 70 mM SDS. The rinsing started at $t = 0$. Plots show adsorbed amount (circles) and thickness of the adsorbed layer (squares) as a function of time.

19 nm, similar to that for the pure emulsion, seen in Figure 3. Relaxation time distributions with a similar appearance were obtained for the LR400/SDS mixtures (not shown). The emulsion-free LR400/SDS complexes had an apparent hydrodynamic radius of 30 nm, but when emulsion droplets were present, the peak was narrow corresponding to an average radius of 18 nm.

As stated above, the cat-guar/emulsion complexes were not fully solubilized until at 70 mM SDS. Figure 11 shows the relaxation time distributions of cat-guar/70 mM SDS mixtures with different amounts of emulsion. There was a shift in the slow mode to longer relaxation times as the amount of silicone oil droplets was increased, see Figure 11a, from 0 ppm (bottom plot) to 50, 100, and finally 400 ppm (top plot). The shift corresponds to a gradual increase in the size of the cat-guar/surfactant complexes from an apparent hydrodynamic radius of 88 to 95 nm with increasing amount of added emulsion.

The progressive addition of emulsion to the corresponding cat-HEC mixture, LR30M/70 mM SDS, gave a different result. Figure 11b shows that the slow mode shifted to shorter relaxation times with an increasing concentration of silicone droplets. This corresponds to a decrease in the hydrodynamic radius from 54 to 20 nm. As in Figure 10, we note that the final apparent size is that of a silicone

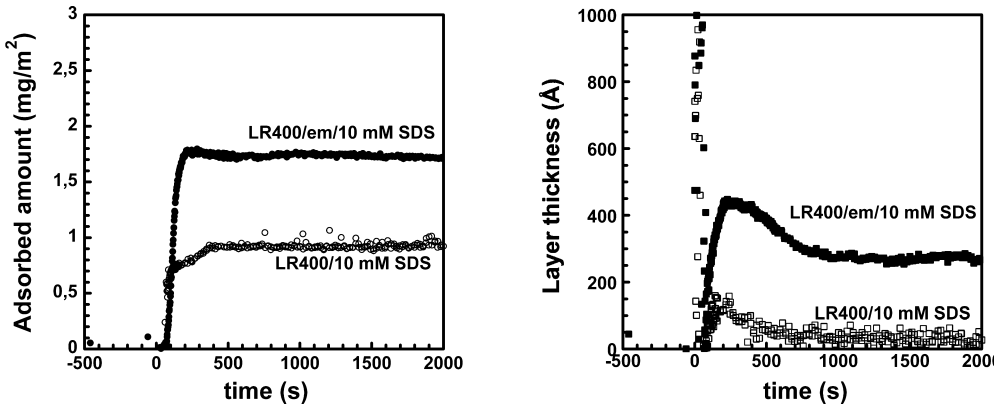

FIGURE 8. Results from adsorption of cat-HEC LR400/SDS solutions with (filled symbols) or without (unfilled symbols) silicone oil emulsion on silica surface followed by dilution of bulk solution with 1 mM NaCl (rinsing). Initial concentrations were 100 ppm polyelectrolyte, 0 or 400 ppm emulsion, and 10 mM SDS. The rinsing started at $t = 0$. Plots show adsorbed amount (circles) and thickness of the adsorbed layer (squares) as a function of time.

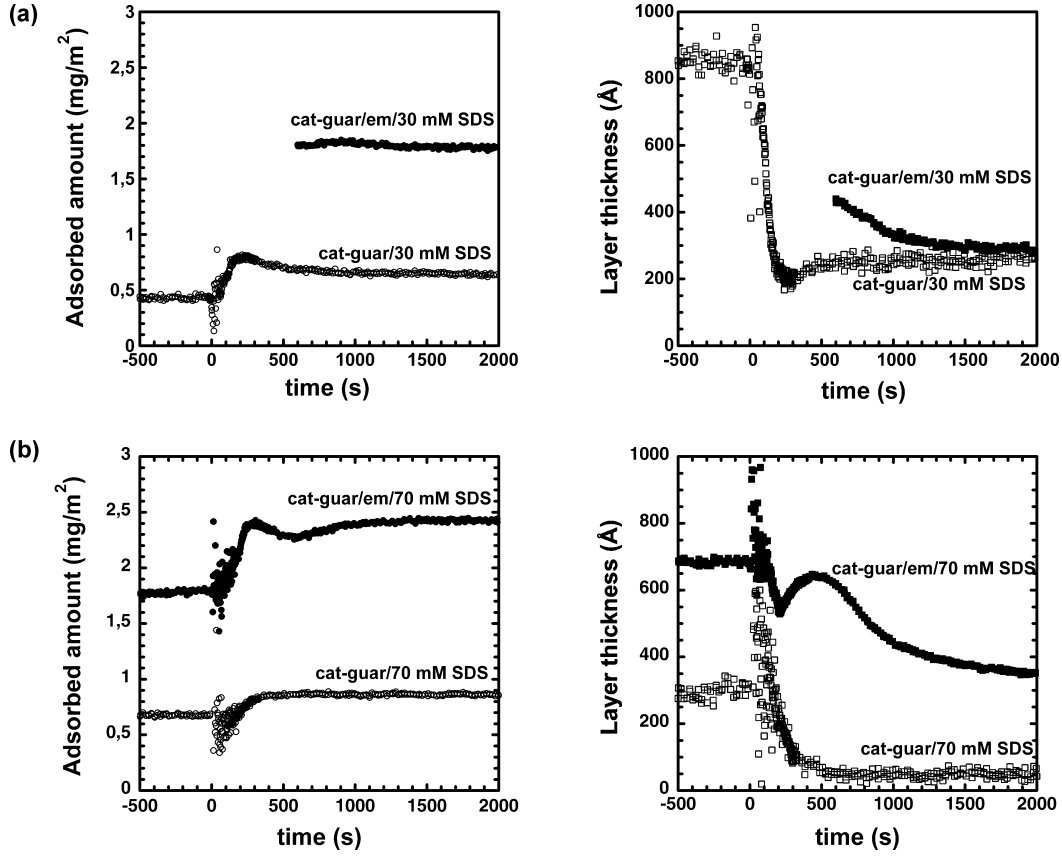

FIGURE 9. Results from adsorption of cat-guar/SDS solutions with (filled symbols) or without (unfilled symbols) silicone oil emulsion on silica surface followed by dilution of bulk solution with 1 mM NaCl (rinsing). Initial concentrations were 100 ppm polyelectrolyte, 0 or 400 ppm emulsion, and (a) 30 or (b) 70 mM SDS. The rinsing started at $t = 0$. Plots show adsorbed amount (circles) and thickness of the adsorbed layer (squares) as a function of time. (The mixture 100 ppm cat-guar/400 ppm emulsion/30 mM SDS was turbid, see text.)

droplet. There was also a narrowing of the slow-mode relaxation time distribution for cat-HEC.

DISCUSSION

Phase Separation and Surface Adsorption Reflect Polyion−Surfactant Interactions. We have previously reported a close correlation between the phase behavior (a phase separation followed by redissolution) of a solution of a cationic polymer, and the observed surface adsorption (enhanced adsorption followed by desorption) from this solution, on the progressive addition of an anionic surfactant (3). The maxima in turbidity and adsorption occurred at the same surfactant concentration. This was observed for all tested combinations of polyion and surfactant. It was concluded that the reason for this relation between solution and interfacial behavior is that both phenomena reflect essentially the same surfactant binding isotherm. The surfactant starts to form aggregates at the polyion at the critical association concentration *(cac)*. A strong interaction between the polyion and the surfactant

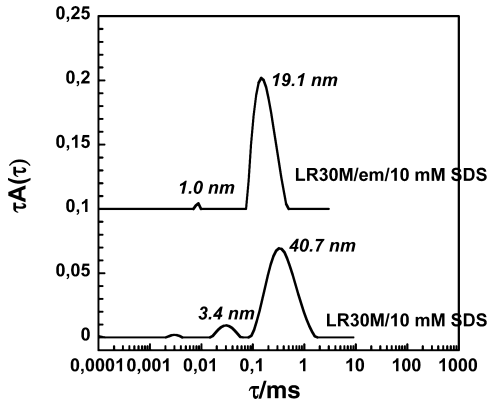

FIGURE 10. Relaxation time distributions at $\theta = 90°$ for 100 ppm cat-HEC LR30 M in 10 mM SDS with (top) and without (bottom) 400 ppm silicone emulsion. Apparent hydrodynamic radii as calculated from the Stokes–Einstein relationship (eq 4) are inserted.

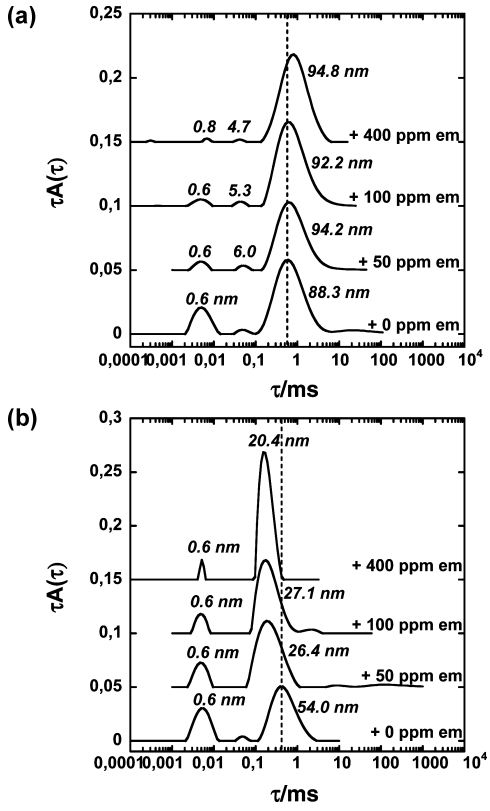

FIGURE 11. Relaxation time distributions at $\theta = 90°$ for 100 ppm (a) cat-guar or (b) cat-HEC LR30 M in 70 mM SDS containing indicated amounts of silicone emulsion. Apparent hydrodynamic radii as calculated from the Stokes–Einstein relationship (eq 4) are inserted.

results in a low cac (15). The surfactant binding eventually leads both to a phase separation and to an enhanced adsorption of complexes at a solid surface. If there is, in addition to the electrostatic interaction, a hydrophobic interaction between the polyion backbone and the surfactant tail, excess surfactant can bind cooperatively to the neutral polyion-surfactant complex at the hydrophobic or the second cac (cac(2)) (16, 17). The overcharging by excess surfactant may lead to a redissolution of the complex and a desorption from a surface (3, 16, 18, 19). The complex is efficiently dissolved if the hydrophobic interaction is strong (3). The positions of the cac and the cac(2) are determined by the strength of the electrostatic and hydrophobic interactions between the surfactant and the polyion, and by the hydrophobic–hydrophilic balance of the surfactant itself, as reflected in its critical micelle concentration (cmc). Generally, if the surfactant is changed, both cac and cac(2) shift in the direction of the shift in the cmc (16).

The results from the present study confirm the correspondence between phase separation and surface adsorption characteristics, not only for mixtures of a cationic polymer and an anionic surfactant, but also for the considerably more complex mixtures where also nonionic surfactant and/or emulsion droplets are present. The surfactant $C_{12}BS$, with a lower cmc than SDS, shifts the adsorption and turbidity peaks to lower concentrations compared to SDS. Addition of nonionic surfactant gives an onset of surface adsorption and phase separation at an even lower $C_{12}BS$ concentration (Figure 4a, c). Including emulsion droplets in the solution with surfactant and cationic polymer gives a dramatic broadening of both the phase separation region and the region of enhanced adsorption. We will now proceed to discuss these results in some detail.

Delivery of the Silicone Oil Emulsion to a Polyion Coated Surface. Progressive addition of the silicone oil emulsion to a surface with preadsorbed cationic polymer resulted in large adsorbed amounts, up to 8 mg/m^2, see Figure 4a. From the huge difference between these results and the results from adding only the surfactant mixture of the emulsion, there can be little doubt that there was a deposition of emulsion droplets. The anionic emulsion droplets have a high affinity to the surface because of electrostatic and hydrophobic interactions between the cationic polymer layer on the silica and the anionic surfactants on the silicone oil droplets. As has previously been inferred from similar experiments on mixtures of just cationic polymer and anionic surfactant (12), there may also be additional deposition of cationic polymer from the bulk solution. The thickness of the adsorbed layer with emulsion droplets is 100 nm, see Figure 4b, which is the same thickness as obtained after adding the pure surfactant $C_{12}BS$. Rinsing with 1 mM NaCl results in only a limited decrease in the adsorbed amount from the emulsion formulation (Figure 4a). This demonstrates that the deposited silicone oil droplets interact strongly with the polyions on the surface. However, the silicone oil droplets desorb by subsequent rinsing with 50 mM SDS, and then the layer swells to 100 nm. The same final layer characteristics were obtained for adsorbed layers formed from the polyelectrolyte solution with added $C_{12}BS$ or the $C_{12}BS/C_{12}E_{23}$ mix. We note that the final layer thickness after rinsing with SDS corresponds to the size of a dissolved LR30M/SDS complex in the bulk at high SDS concentrations (see Figure 10 and, for data at 50 mM SDS, ref 3). At least a fraction of the adsorbed LR30 M is practically irreversibly attached, and the thickness of the maximally swollen layer seems to be determined by the size of the surfactant-swollen polyion chains.

Analogy between Binding to Silica and to Emulsion Droplets. There seems to be a close analogy

between the binding of a cationic polymer in the presence of added surfactant to a silica surface and to a negatively charged emulsion droplet. Both cases represent interactions with anionic surfaces. A comparison of the solubility of the polyion/emulsion complexes in Figure 6 with the adsorption data of the same polyions in Figure 2a supports this idea. Over a considerable low-concentration range of added SDS in Figure 6, the polyion−droplet interaction seems unaffected by the surfactant. This is quite similar to the adsorption results in Figure 2a where the adsorbed amount from a 100 ppm polyelectrolyte solution is unaffected at low surfactant concentrations. The polyion−droplet complexes start to dissociate (Figure 6), seen as an onset of a decrease in turbidity, at SDS concentrations very similar to the respective adsorption maxima in Figure 2a. In both cases, the dissociation of the polyion−droplet complexes from the surfaces or particles should be due to the formation of soluble polyion/SDS complexes by the binding of excess SDS to the polyions. We note that the complete dissolution of the polyion−droplet complexes, seen as a leveling off of the turbidity, occurs at a much higher SDS concentration for cat-guar than for cat-HEC, again in accordance with the trends for the decrease in the adsorbed amount in Figure 2a. Hence, there are qualitative similarities between adsorption to silica and binding to emulsion droplets. This suggests that we may use the results from adsorption experiments on macroscopic model surfaces as a guide to how polyion−surfactant ion complexes interact also with mesoscopic particle surfaces.

The results from Figure 6 may, furthermore, help us to understand both the striking turbidity curves of Figures 4c and 5, when emulsion is added to 100 ppm solutions of the various polyions, and the wide composition range of enhanced adsorption seen in Figure 4a for the experiment where emulsion is added to a solution of cat-HEC LR30M. The mentioned turbidity curves all show a dramatic time-dependent drop in turbidity at high emulsion concentrations. The turbidity drop in Figure 5 occurs at an emulsion content equivalent to 30 mM C_{12}BS for cat-HEC, but significantly higher (40−50 mM) for cat-guar. On the basis of the results from Figure 6, we suggest that the redissolution of the droplet/polyion/surfactant complexes occurs at conditions when the concentration of free surfactant, accompanying the surfactant adsorbed to the droplets in the emulsion, reaches cac(2), so that soluble polyion−surfactant ion complexes detach from the droplet surfaces. The final redissolution seen in Figures 4c and 5 is then caused by the same mechanism both in the presence and absence of emulsion droplets, but when the emulsion droplets are present, they consume most of the added surfactant and considerably widen the phase-separation area in terms of the total surfactant concentration. The difference between cat-guar and cat-HEC in Figure 5 supports this conclusion, with a significantly higher cac(2) and a more gradual surfactant-binding occurring for cat-guar. The same mechanism explains the wide range of emulsion concentrations giving an enhanced adsorption in Figure 4a.

We then arrive at the following tentative interpretation of the events occurring on adding emulsion to a 100 ppm cationic polymer solution. Close to the cac of the droplet-free surfactant mixture, polyion/surfactant/droplet complexes are formed (see the onset of enhanced turbidity in Figure 4c). At the onset of the turbidity increase in Figures 4c and 5 we have the following composition of the system: There is a significant excess of anionic C_{12}BS surfactant (0.1 mM) relative to the concentration of cationic polymer charges (0.06 mM). On the other hand, with a weight-average molecular weight of 1×10^6 for the polyion and assuming a polydispersity of roughly 2, there is a 20-fold excess of polyion molecules compared to the number of emulsion droplets. The structure of the polyion/surfactant/droplet complex formed is unknown, but the turbidity suggests that a large number of polyion molecules are involved in a dispersed complex. As the concentration of emulsion is increased, both the turbidity and the adsorption data indicate that more droplets are added to the complexes. However, at sufficiently high concentrations, the concentration of free surfactant ions accompanying the emulsion reaches cac(2), so that polyion−surfactant ion complexes with an excess of bound surfactant start to detach from each other and from the emulsion droplets. This results in a decreasing turbidity, finally approaching that of the polyion-free dilute emulsion.

Droplet−Polyion Interactions in Redissolved Formulations. The detailed information from DLS measurements on bulk solutions of polyelectrolyte/emulsion/SDS at high SDS concentrations confirm the picture given above, and reveal differences in the aggregation between polyions and droplets for cat-guar and cat-HEC at similar SDS concentrations. Let us first consider the situation at 70 mM SDS. This SDS concentration is where a total redissolution of cat-guar just occurs, but far above the redissolution conditions for cat-HEC. The relaxation time distribution for a cat-guar/70 mM SDS mixture is shown in Figure 11a (bottom plot), and contains peaks corresponding to surfactant micelles ($R_{app,h}$ = 1 nm) and to large polyion−surfactant ion complexes ($R_{app,h}$ = 88 nm), the latter of a size suggesting single polyion molecules dressed with surfactant micelles. There is a gradual shift of the broad peak to longer relaxation times on adding increasing amounts of emulsion. This corresponds to an increase in the size of the complex (from $R_{app,h}$ = 88 to $R_{app,h}$ = 95 nm). Presumably, the cat-guar/surfactant complexes swell because of the incorporation of silicone droplets, implying a binding of the silicone droplets to the cat-guar polyions. The association between silicone droplets and cat-guar under these conditions is consistent with the observation that a mixture of cat-guar with 70 mM SDS adsorbs to hydrophilic (anionic) silica surfaces (Figure 9b, conditions prior to rinsing), if we make the analogy between adsorption to a negative silica surface and binding to a negatively charged emulsion droplet.

The corresponding measurement with increasing amounts of emulsion to a mixture of cat-HEC/70 mM SDS (Figure 11b) shows a different result. There is a narrowing of the broad

peak and a shift to faster relaxation times. The results suggest that in this mixture, the droplets and the polyion−surfactant ion complexes give rise to separate peaks, which are superimposed, and that the stronger scattering from the dense silicone oil droplets gradually takes over, to dominate the scattering completely at the final concentration of 400 ppm. This implies that the polyions and silicone oil droplets are not aggregated, which is consistent with the fact that mixtures of cat-HEC with SDS do not adsorb to hydrophilic (anionic) silica surfaces at 70 mM SDS (Figure 7c, conditions prior to rinsing).

Mixtures of cat-HEC (LR30M) with 10 mM SDS are close to the redissolution conditions for this polyelectrolyte−surfactant pair. The relaxation time distribution for this mixture in the absence of emulsion (Figure 10) shows two peaks which correspond to surfactant micelles ($R_{app,h} = 1$ nm) and polyion-surfactant ion complexes ($R_{app,h} = 40$ nm), respectively. Just as at 70 mM SDS, however, the addition of silicone droplets to the mixture gives a narrow peak with an $R_{app,h}$ of 18 nm, which is the size of a silicone droplet. This indicates that the polyion−surfactant ion complexes do not associate to the droplets at this concentration, which again is consistent with the absence of adsorption, under these conditions, of the polyion−surfactant ion complexes at silica surfaces, see the initial conditions in Figure 7a.

Delivery of the Emulsion to Anionic Surface by Diluting Full Formulation. Before discussing the results of the rinsing procedure, we note that no deposition prior to rinsing was observed in any of the experiments accounted for in Figures 7 and 8, whereas the ellipsometry results in Figure 2 clearly reveal the presence of an adsorbed layer of surfactant-swollen polyion−surfactant ion complexes at the corresponding bulk contents of polyelectrolyte and surfactant. These apparently conflicting results agree with previous observations of the history-dependent, nonequilibrium nature of deposited polyion−surfactant ion complexes (11–13). More specifically, sufficiently net negatively charged polyion−surfactant ion complexes do not adsorb to a virgin negatively charged silica surface, as shown in Figures 7 and 8. On the other hand, a layer of preadsorbed cationic polymers is very difficult to remove completely from the silica surface by adding even very large amounts of a complexing anionic surfactant, as shown in Figures 2 and 4.

Turning now to the results of the rinsing procedure, Figures 7−9 show that the polyions differ regarding their capacity to deliver premixed polyelectrolyte/emulsion/SDS mixtures to hydrophilic silica. Moreover, the delivery depends on the concentration of surfactant present in the initial formulation. Both these findings have important implications for making silicone delivery formulations in applications. On the basis of the analysis given above, we are now in a position to understand these differences. Adsorption will occur if the complexes manage to attach to the surface, with the polyion acting as a cationic bridge between the anionic silica surface and the anionic droplets. This is not obvious because the polyion exists in the form of redissolved polyion−surfactant ion complexes in the bulk. The soluble bulk complexes are overcharged to various degrees depending on both the amount of excess surfactant, and the capacity of the polyion to bind excess surfactant. Adsorption from the premixed solutions to hydrophilic silica occurred for the purified cat-guar (Figure 9), but not for the cat-HECs (Figures 7 and 8). The basic principle of delivery by dilution is that surfactant molecules will detach from the polyion−surfactant ion complexes during dilution and thus bring the system into a state of association and phase separation. During the rinse with 1 mM NaCl, a steep increase in adsorption was observed for the cat-guar and the cat-HEC mixtures, but the extent of the increase depended on the initial surfactant concentration. The further away from phase separation the system, the smaller the increase in adsorbed amount. In many cases, we also observed a transient peak in adsorption during dilution. The simplest explanation to this transient peak was that the system is gradually taken through a path corresponding to a reverse of that shown in Figure 2a, that is, as the surfactant concentration is lowered, there should eventually be a decrease in the adsorbed amount.

For cat-HEC, it was observed that the adsorption on rinsing is stronger when we started close to redissolution conditions (Figure 7). Between 10 mM and 30 mM SDS, there was a large difference especially in the delivery of silicone oil droplets, as evaluated from the difference in adsorbed amount with and without the presence of emulsion. At still higher SDS concentration, there was a poor delivery also of polyion−surfactant ion complexes on rinsing. Optimal conditions for efficient delivery are apparently when the system is close to the redissolution conditions, so that already a slight dilution will bring the system into a situation where the polyion-surfactant ion complexes stick to each other and to all surfaces (droplets and substrate silica). If the initial conditions are at surfactant concentrations high above what is required for redissolution, most of the material may simply be washed away during rinsing, so that the formulation becomes too dilute when, finally, the conditions of association and phase separation are reached.

To reach the most favorable conditions for delivery, there seem to be the following options. Either one can adjust the initial surfactant concentration, to be just above redissolution conditions, or if other requirements restrict the choice to a high initial surfactant concentration, one can change the polyion to one that is less efficient in binding excess surfactant−for instance, from cat-HEC to cat-guar−so that the system in this way is tuned to conditions close to redissolution. A third possible option is to change the surfactant, or possibly introduce a cosurfactant. In this way, one can also tune the surfactant concentration where redissolution occurs.

CONCLUSIONS

It is possible to deliver anionic silicone oil droplets to an anionic surface by cationic polymers. These silicone oil droplets strongly adsorb to a preadsorbed cationic polymer layer on the anionic surface. The adsorbed droplets remain

on rinsing with a dilute electrolyte solution, but can be removed by rinsing with SDS, leaving a swollen layer of polyion/SDS complexes.

The adsorbed amount obtained on silica from a mixture of cationic polymer/emulsion/surfactant depends to a large extent on the characteristics of the cationic polymer, and also on the amount of surfactant present in the formulation. We have shown that the hydrophobicity of the polyion determines the solubility of the polyion−surfactant ion complex, which indirectly affects the drive for adsorption. A cationic polymer with a low hydrophobicity (cat-guar in the present case) forms polyion−surfactant ion complexes that do not redissolve as easily, because of a poor binding of excess surfactant. The result is a high turbidity in bulk solutions, and a high adsorption in rinse experiments. The results imply that the highest adsorption is obtained in mixtures close to phase separation, and that the solubility is governed by the polymer hydrophobicity. These conclusions will be further tested in a future study in this series.

There is a close analogy between aggregation of the cationic polymer/anionic surfactant complex with emulsion droplets and the adsorption of the same complex to an anionic silica surface. Redissolution of polyion/emulsion complexes in the bulk and desorption from the surface occur at the same free surfactant concentrations, indicating that the processes are governed by the polyion/surfactant binding isotherm.

Particles, such as emulsion droplets, present in the formulation may consume a significant fraction of the surfactant molecules, thereby increasing the range of surfactant concentrations where polyion−surfactant ion complexes associate to each other and to surfaces, resulting in phase separation and surface deposition.

Acknowledgment. Alexandra Andersson, Biochemistry, Lund University, is gratefully acknowledged for the investigation of the cat-guar with BCA assay. Karin Schillén and David Lööf, Physical Chemistry 1, Lund University, are gratefully acknowledged for valuable discussions and assistance during the DLS experiments. Ronita Marple, Beauty Analytical, Procter & Gamble, is gratefully acknowledged for the GPC-LS analysis of the polyions. This study was supported by The Procter & Gamble Company.

REFERENCES AND NOTES

(1) Yahagi, K. *J. Soc. Cosmet. Chem.* **1992**, *43*, 275–284.
(2) Berthiaume, M. D.; Jachowicz, J. *J. Colloid Interface Sci.* **1991**, *141*, 299–315.
(3) Svensson, A. V.; Huang, L.; Johnson, E. S.; Nylander, T.; Piculell, L. *ACS Appl. Mater. Interfaces* **2009**, *1* (11), 2431–2442.
(4) Essafi, W.; Poulin, P.; Chiron, S.; Bavouzet, B. *Langmuir* **2004**, *20*, 123–128.
(5) Bibette, J.; Morse, D. C.; Witten, T. A.; Weitz, D. A. *Phys. Rev. Lett.* **1992**, *69*, 2439–2442.
(6) Gruber, J. V.; Lamoureux, B. R.; Joshi, N.; Moral, L. *J. Cosm. Sci.* **2001**, *52*, 131–136.
(7) Gruber, J. V.; Lamoureux, B. R.; Joshi, N.; Moral, L. *Colloids Surf. B* **2000**, *19*, 127–135.
(8) Marchioretto, S.; Blakely, J. *SOFW J.* **1997**, *123*, 811–812, 814−816, 818.
(9) Seaman J. K. In *Handbook of Water-Soluble Gums and Resins*; Davidson, R. L., Ed.; McGraw-Hill: New York, 1980; Chapter 6.
(10) Tiberg, F.; Landgren, M. *Langmuir* **1993**, *9*, 927–931.
(11) Shubin, V. *Langmuir* **1994**, *10*, 1093–1100.
(12) Terada, E.; Samoshina, Y.; Nylander, T.; Lindman, B. *Langmuir* **2004**, *20*, 1753–1762.
(13) Terada, E.; Samoshina, Y.; Nylander, T.; Lindman, B. *Langmuir* **2004**, *20*, 6692–6701.
(14) Jansson, J.; Schillén, K.; Olofsson, G.; Cardoso da Silva, R.; Loh, W. *J. Phys. Chem. B* **2004**, *108*, 82–92.
(15) Anthony, O.; Zana, R. *Langmuir* **1996**, *12*, 1967–1975.
(16) Sjöström, J.; Piculell, L. *Colloid Surf., A* **2001**, 183–185, 429−448.
(17) Lynch, I.; Sjöström, J.; Piculell, L. *J. Phys. Chem. B* **2005**, *109*, 4258–4262.
(18) Guillemet, F.; Piculell, L. *J. Phys. Chem.* **1995**, *99*, 9201–9209.
(19) Goddard, E. D.; Hannan, R. B. *J. Am. Oil Chem. Soc.* **1977**, *54*, 561–566.

AM9006319